DEVELOPMENT OF A SIX-COMPONENT BALANCE FOR MEASUREMENTS OF FORCES AND MOMENTS ACTING IN IMMERSED CYLINDERS

Ivan Korkischko
NDF, Departamento de Engenharia Mecânica da Escola Politécnica da Universidade de São Paulo, São Paulo, Brazil
ivan.korkischko@poli.usp.br

Julio R. Meneghini
NDF, Departamento de Engenharia Mecânica da Escola Politécnica da Universidade de São Paulo, São Paulo, Brazil
jmeneg@usp.br

Kazuo Nishimoto
TPN, Departamento de Engenharia Naval e Oceânica da Escola Politécnica da Universidade de São Paulo, São Paulo, Brazil
kazuo.nishimoto@poli.usp.br

Gustavo S. Ássi
NDF, Departamento de Engenharia Mecânica da Escola Politécnica da Universidade de São Paulo, São Paulo, Brazil
gustavo.assi@poli.usp.br

Abstract. *The measurement of forces and moments acting on a body immersed in a current is one of the most important issues of measurement in fluid mechanics. In this paper, the design of a six-component balance, employed to measure the hydrodynamic forces acting on a bluff body, is shown. Six-component balances can be internals, mounted inside the model, or externals, located outside the tests section. The six-component balance developed and described in this work is of the external type, and will be fixed mounted in a traverse system. One particular transducer geometry is shown and its calibration discussed. After evaluate the acting loads (forces and moments), the finite element analysis software (FEA) is employed to determine the construction material. A modal analysis has been used for the determination of natural frequencies, and a static analysis for the determination of stress and strain. Aluminium 5052 has been chosen for the balance. Knowing the construction material, the finite element code has been employed to simulate the complete procedure of calibration and to obtain a preliminary-numerical calibration matrix of six degrees of freedom. This calibration matrix decouples the different components of the simultaneous acting loads. One of the advantages of the adopted geometry is the necessity of a lower number of strain gages – 16 – comparing to others geometries. The balance design and calibration procedure is described in this paper.*

Keywords*: six-component balance, transducer, finite element analysis software, calibration matrix, strain gage*

1. Introduction

The design and calibration procedure of a six-component balance, employed to measure hydrodynamic forces and moments, is shown in this paper. The measurement of forces and moments acting on a circular-cylinder immersed in a current is one of the most important issue of measurement in fluid mechanics. In this work, the balance is employed to measure the hydrodynamic forces acting on a bluff body. The instrument used for this task is a six-component balance, also known as six-component load cell. Six-component balances can be internals, mounted inside the model, or externals, located outside the tests section. The six-component balance developed and described here is of the external type, and will be fixed mounted in a traverse system. The concept of whole experimental apparatus has been developed to be employed in experiments of vortex-induced vibration (VIV) on bluff bodies. The balance design proposed by Nishimoto (1985) and shown in "Fig. 1" has been chosen.

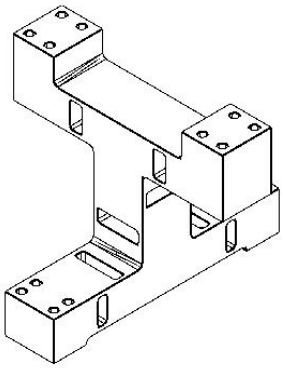

Figure 1. Transducer geometry proposed by Nishimoto (Nishimoto, 1985)

2. Project parameters

The project of the six-component balance has obeyed some parameters imposed by the tests that will be performed in the re-circulating water channel recently installed at the University of São Paulo. This water channel has been designed to carry out investigation concerning vortex shedding and vortex-induced vibration. The equipment is part of the experimental facilities of NDF ("Núcleo de Dinâmica e Fluidos"), located at the Department of Mechanical Engineering, "Escola Politécnica". The test section of that channel (Fig. 2) imposes the following parameters for the design of the six-component balance: $a = 0.8m$, $b = 0.6m$, and maximum current speed $U = 1.0m/s$.

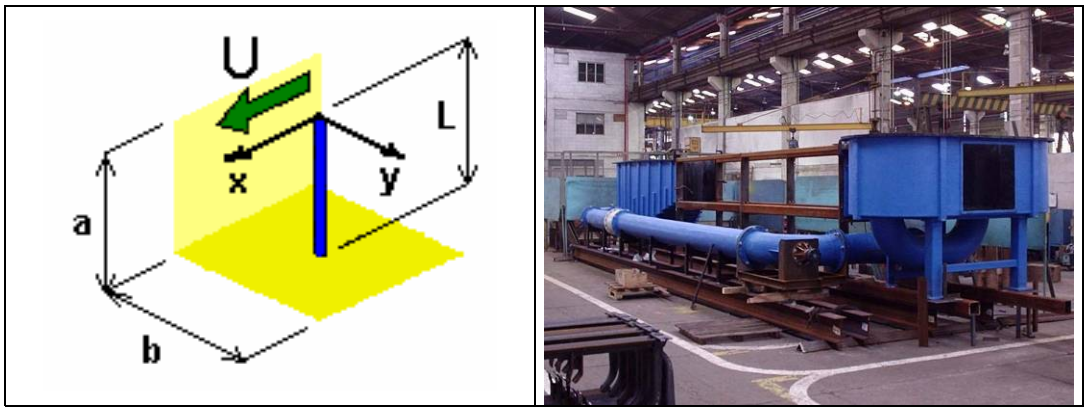

Figure 2. (a) Diagram of the test section of the re-circulating water channel; (b) Photo of the assembling of the re-circulating water channel.

The water channel will be employed to measure hydrodynamic forces of oscillating circular-cylinders and general bluff bodies. The circular-cylinders that will be tested have the following geometrical characteristics: $L = 0.8m$ (length) and $D_{\max} = 0.1m$ (maximum diameter). The hydrodynamic coefficients have been admitted as $C_d = 1.2$ (mean drag coefficient – fixed cylinder), and $C_l = 1.0$ (amplitude of lift coefficient – fixed cylinder). The cylinder experiences when oscillating a drag and lift amplification for a certain range of reduced velocity ($V_r = U / f_n D$). This fact must be taken into account during the balance design period. In our case, C_d and C_l have been admitted to be increased by a factor of about five when the cylinder is oscillating. Following the work by Khalak and Williamson (1999), the maximum hydrodynamic coefficients have been considered as $C_{d\max} = 5.2$, and $C_{l\max} = 3.0$.

2.1. Natural oscillatory frequency of the cylinder

In order to avoid the balance to oscillate in the frequency of the oscillating cylinders to be tested, the natural frequencies of the balance have to be well above the oscillating frequencies. In vortex-induced vibration experiments is common to define the reduced velocity by the following expression (Meneghini, 2002):

$$V_r = \frac{U}{f_n D} \tag{1}$$

where V_r is the reduced velocity, U is the free-stream velocity, f_n is the natural oscillatory frequency of the cylinder, and D is the cylinder diameter.

From the ranges of free-stream velocities, reduced velocities, and the cylinder diameters, the range of oscillatory frequency can be found as

$$f_n = \frac{U}{V_r D} \tag{2}$$

In this paper, the following ranges of U, V_r and D, have been considered: $0.1m/s < U < 1.0m/s$, $1 < V_r < 16$, and $0.02m < D < 0.1m$. With these values, the interval of frequency can be estimated by expression (2) and is found to be $0.063Hz < f_n < 50Hz$. The balance has been designed to have its first natural period at least 10 times higher than the maximum oscillatory frequencies of the cylinders to be tested.

2.2. Evaluation of the acting loads in an immerse cylinder

The most important phase of the balance design is the evaluation of the acting forces and moments on the cylinder to be tested. These parameters define the transducers and strain-gages to be employed in the equipment. This evaluation employed the tests parameters.

2.2.1. Forces

The maximum forces are evaluated considering the definitions of the hydrodynamic coefficients *Cd* and *Cl*, and a security factor (SF):

$$F_{x_{\max}} = \frac{1}{2} C_{d\max} \rho_{H_2O} U^2 DL(SF) \tag{3}$$

$$F_{y_{\max}} = \frac{1}{2} C_{l\max} \rho_{H_2O} U^2 DL(SF) \tag{4}$$

In these expressions, ρ_{H2O} is the water specific mass, U is the current speed, and L is the cylinder length. The security factor has been chosen equal to 2. With equations (3) and (4) and the ranges of velocity shown in section 2.1, the maximum forces that the six-component balance should handle are:

$F_{x_{\max}} = 416N$

$F_{y_{\max}} = 240N$

2.2.2. Moments

The uniform distribution of the drag and lift loads result in the following values of the acting moments:

$M_{x_{\max}} = 96Nm$

$M_{y_{\max}} = 166Nm$

3. Material selection

Aluminum has been chosen as the material for the balance. The following properties of aluminium have been employed for the stress analysis employing the finite element method: $E = 70GPa$ (elasticity module), $\upsilon = 0.33$ (Poisson's coefficient), and $\rho_{al} = 2700kg/m^3$. The material model adopted was an elastic, linear and isotropic material (Gere, 2003). In order to evaluate the natural frequencies of the balance, a modal analysis – determination of natural frequencies, and static analysis have been carried out employing the commercial code ANSYS. With the loads determined in the previous section, ANSYS have been used to determine the stress and strain in the balance. In Fig. 3, the mesh employed in the calculations and the static results are shown. With this analysis, the following parameters have been determined:

$f_n = 492Hz$
$\sigma_{\max} = 95,4MPa$
$\varepsilon = 0.885 \cdot 10^{-3}$

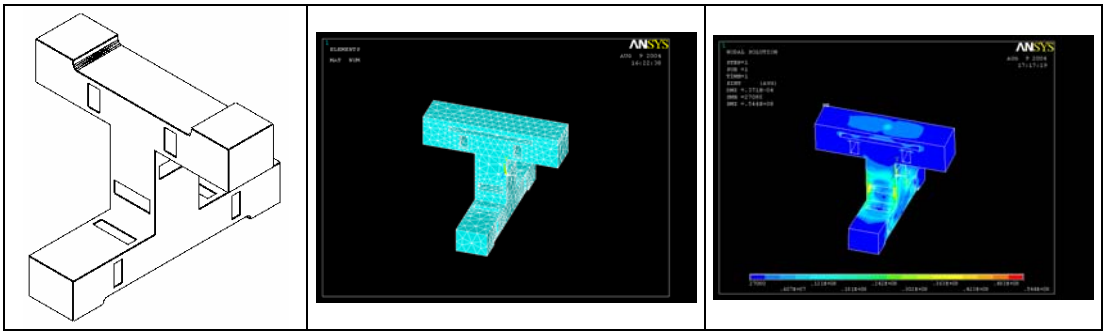

Figure 3. (a) Simplified transducer geometry, (b) FEA mesh of the simplified transducer geometry, (c) Static analysis result of the simplified transducer geometry

Consulting the main suppliers of aluminium, the 5052 aluminium alloy has been selected. The main characteristics and properties (ASM, 1979) of this alloy are:

- Used in the construction of structures,
- Good mechanic resistance,
- High corrosion resistance,
- Good conformability,
- High fatigue resistance.

4. Strain gages

The resistance strain gage is based on the principle that the electrical resistance of a conductor depends on its shape. The basic relationships between resistance change and shape are shown in "Eq. 5".

$$R = \rho \frac{L}{A} \tag{5}$$

where R is the resistance, ρ is the resistivity constant of the conductor material, L is the conductor length, and A is the cross-sectional area.

The strain sensitivity, or gage factor F, that describes the resistance change of a conductor in relation to the length change (Considine, 1993), can be defined as

$$F = \frac{\Delta R / R}{\Delta L / L} \tag{6}$$

5. Construction and mounting

Trying to save material and, consequentially, financial resources, the transducer was milled in two pieces: a main part, shown in “Fig. 4.a” and another superior piece depicted in “Fig. 4.b”. A mill and a lathe were employed for this task.

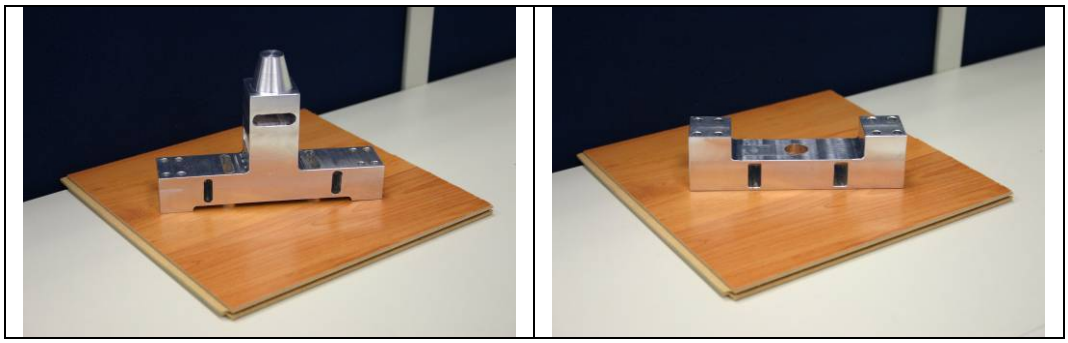

Figure 4. (a) Main piece of the transducer, (b) Superior piece of the transducer

The conic member in each piece of the transducer transfer the total load that act in the superior piece, “Fig. 4.b”, to the main piece, “Fig. 4.a”. These two pieces were glued together with an epoxy adhesive after the milling process. This method of union was chosen because the resulting transducer formed by the two pieces would act as it was milled from a single block of aluminium. Then, the strain gages were attached to specific points of the transducer surface “Fig. 5”.

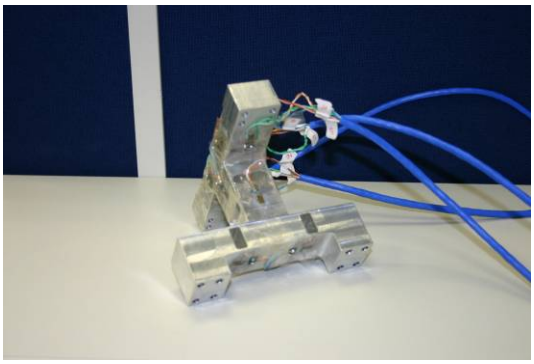

Figure 5. Six-component balance mounted: pieces glued together and strain gages attached

6. Calibration and calibration matrix

Prior to the experimental calibration procedure and in order to allow a better understanding of the calibration matrix concept, the necessary steps to obtain the calibration matrix have been numerically simulated. Formerly, strains were obtained by FEA simulations of the isolated loads (F_x, F_y, F_z, M_x, M_y and M_z) applied to the transducer. With the strain values, it was possible to mount Wheatstone bridges, which have been employed for the data acquisition. The calculated electrical tensions were used to form the calibration matrix. The following procedures demonstrate how to calibrate and obtain the calibration matrix of a six-component balance. The experimental calibration procedure is analogous to the numerical procedure presented in this paper.

6.1 Wheatstone bridges

The electrical signals of the strain gages are associated in Wheatstone bridges of four and two active arms. One active arm is composed of one strain gage. “Fig. 6” illustrates a Wheatstone bridge circuit. In the experimental calibration, the Wheatstone bridges voltage outputs will be directly measured and used to form the calibration matrix.

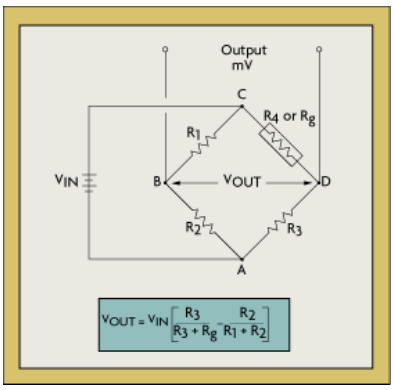

Figure 6. Wheatstone bridge circuit (Omega Engineering, 2004)

6.2 Isolated loads

After applying increasing isolated loads (F_x, F_y, F_z, M_x, M_y and M_z) and measuring the Wheatstone bridges outputs, it is possible to obtain the electrical tension coefficients that form the vectors $\{e\}$ for each isolated load.

6.3 Calculation of the calibration matrix

From Hooke's law to elastic-linear materials, it can be found the following expression:

$$\{e\} = [C]\{F\} \tag{7}$$

The matrix $[C]$ is composed by the $\{e\}$ vectors, where each of vectors $\{e_{Fx}\}$, $\{e_{Fy}\}$, $\{e_{Fz}\}$, $\{e_{Mx}\}$, $\{e_{My}\}$ and $\{e_{Mz}\}$ form one of the six columns of the matrix $[C]$, which has 6x6 dimension.

The inverse of the matrix $[C]$ is the calibration matrix $[C]^{-1}$.

Thus,

$$\{F\} = [C]^{-1}\{e\} \tag{8}$$

where:

$\{F\}$: loads (forces and moments) vector

$\{e\}$: Wheatstone bridges outputs vector

References of calibration and calibration matrix can be found at (Ewald, 2000), (Fernandez *et al*, 2001), (Liu and Tzo, 2002), (Giesecke *et al*), (Cambay, Ersoy and Tankut, 2004), (Cigada, Falco and Zasso, 2001), (Bicchi) and (Flayi and Vuletich, 1995).

6.4 Numerical simulation of the calibration matrix

As an example of the process of obtaining the calibration matrix, the numerical simulation matrix is shown in this section. The following loads where applied into the finite element analysis transducer geometry:

$$\begin{pmatrix} F_x \\ F_y \\ F_z \\ M_x \\ M_y \\ M_z \end{pmatrix} = \begin{pmatrix} 500N \\ 500N \\ 500N \\ 400Nm \\ 200Nm \\ 200Nm \end{pmatrix}$$

The Wheatstone bridges were mounted using the constants:

$R = 120\Omega$

$F = 2(GageFactor)$

$e_0 = 12V$

The Wheatstone bridges outputs were computed for two and four active arms with the following equations

$$e = e_0 \left[\frac{R(\Delta R_1 + \Delta R_4) + \Delta R_1 \Delta R_4}{(2R + \Delta R_1)(2R + \Delta R_4)} \right](V) \quad \text{(two arms)} \tag{9}$$

Four active arms:

$$e = e_0 \left[\frac{R(\Delta R_1 + \Delta R_4 - \Delta R_2 - \Delta R_3) + \Delta R_1 \Delta R_4 - \Delta R_2 \Delta R_3}{(2R + \Delta R_1 + \Delta R_2)(2R + \Delta R_3 + \Delta R_4)} \right](V) \quad \text{(four arms)} \tag{10}$$

With the Wheatstone bridges outputs, the loads vectors $\{e_{Fx}\}$, $\{e_{Fy}\}$, $\{e_{Fz}\}$, $\{e_{Mx}\}$, $\{e_{My}\}$ and $\{e_{Mz}\}$ were found and combined to form the matrix $[C]$:

$$C = \begin{pmatrix} \text{-7,760E-07} & \text{1,640E-07} & \text{3,600E-08} & \text{4,400E-06} & \text{3,500E-08} & \text{1,150E-05} \\ \text{-4,700E-07} & \text{3,200E-08} & \text{-9,780E-07} & \text{-5,700E-06} & \text{-1,250E-07} & \text{8,500E-07} \\ \text{-9,200E-08} & \text{-2,400E-07} & \text{7,480E-07} & \text{3,700E-06} & \text{-4,000E-08} & \text{1,200E-06} \\ \text{1,600E-08} & \text{6,000E-09} & \text{-2,260E-07} & \text{-4,975E-07} & \text{-8,350E-07} & \text{-1,500E-08} \\ \text{-5,580E-07} & \text{1,000E-08} & \text{2,260E-07} & \text{1,550E-07} & \text{9,600E-06} & \text{-1,400E-06} \\ \text{-2,000E-09} & \text{-4,480E-07} & \text{9,600E-08} & \text{1,200E-07} & \text{6,000E-08} & \text{-8,000E-08} \end{pmatrix}$$

The inverse of the matrix $[C]$ is the calibration matrix $[C]^{-1}$.

$$C^{-1} = \begin{pmatrix} \text{465072,12} & \text{-1695160,9} & \text{-3966310,2} & \text{-5347470,1} & \text{-517940,72} & \text{2090796,7} \\ \text{-50456,855} & \text{104708,97} & \text{174068,69} & \text{-949017,31} & \text{-65512,864} & \text{-2350557,9} \\ \text{-166307,16} & \text{679003,78} & \text{335589,67} & \text{-7001670,2} & \text{-595662,96} & \text{-299228,63} \\ \text{6276,3679} & \text{-158311,34} & \text{225200,29} & \text{1517624,2} & \text{131383,9} & \text{-106395,36} \\ \text{47727,829} & \text{-120164,82} & \text{-293376,87} & \text{-299832,69} & \text{74026,229} & \text{163691,53} \\ \text{116573,41} & \text{-56777,309} & \text{-355151,52} & \text{-902258,82} & \text{-82379,475} & \text{214955,77} \end{pmatrix}$$

And, with the "Eq. 8", any applied loads are obtained if the vector $\{e\}$ is known.

7. Conclusions

This paper contains the complete project of a six-component balance, employed to measure the hydrodynamic forces acting on a bluff body. In order to evaluate the natural frequencies of the balance, a modal analysis – determination of natural frequencies, and static analysis, determination of the stress and strain in the balance, have been carried out employing the commercial code ANSYS. With these values, natural frequencies, stress and strain, the material have been selected and the strain gages have been specified. Finally, the procedures of calibration and how to obtain the calibration matrix have been presented including a numerical simulation of the entire procedure.

8. Acknowledgements

The authors would like to acknowledge the support of FAPESP ("Fundação de Amparo à Pesquisa do Estado de São Paulo) and the technical work carried out by the technician Douglas Silva. Also, the support by Micro-Measurements Division (MEASUREMENTS GROUP, INC.) and ALFA Instrumentos Ltda are greatly appreciated.

9. References

ASM – American Society for Metals, 1979, Metal Handbook – Volume 2 – Properties and Selection: Nonferrous Alloys and Pure Metals, Ninth Edition.

Ássi, G. R., 2003, Desenvolvimento de um Canal de Água Circulante para experimentos em dinâmica dos fluidos; XIX Congresso de Iniciação Científica e Tecnológica em Engenharia, XI Simpósio Internacional de Iniciação Científica da USP, São Carlos, 2003.

Bicchi, Antonio; A criterion for optimal design of multi-axis forces sensors.

Canbay, E., Ersoy, U., Tankut, T., 2004, A three component force transducer for reinforced concrete structural testing; Engineering Structures 26, pp. 257-265.

Cigada, A., Falco, M., Zasso, A., 2001, Development of new systems to measure the aerodynamic forces on section models in wind tunnel testing, Journal of Wind Engineering and Industrial Aerodynamics 89, pp. 725-746.

Considine, Douglas M., 1993, Process/Industrial Instruments and Controls Handbook., 4th Edition, McGraw-Hill.

Ewald, Bernd F. R., 2000, Multi-component force balances for conventional and cryogenic wind tunnels; Measurement Science and Technology 11, pp. 81-94.

Fernadez, A., Berghmans, F., Brichard, B., Mégert, P., Decréton, M., Blondel, M., Belchambre, A., 2001, Multi-component force sensor based on multiplexed fibre Bragg grating strain sensors, Measurement Science and Technology 12, pp. 1-4.

Flayi, R.G.J., Vuletich, I.J., 1995, Development of a wind tunnel test facility for yacht aerodynamic studies, Journal of Wind Engineering and Industrial Aerodynamics 58, pp. 231-258.

Gere, James M., 2003, Mecânica dos Materiais, Pioneira Thomson Learning, São Paulo.

Giesecke, P., Polansky, L., Müller, F., Theiss, D., Six-Component Underfloor Balance.

Khalak, A., Williamson, C. H. K., 1999, Motions, forces and mode transition in vortex-induced vibrations at low mass-damping, Journal of Fluids and Structures 13, pp. 813-851.

Liu, Sheng A., Tzo, Hung L., 2002, A novel six-component force sensor of good measurement isotropy and sensitivities, Sensors and Actuators A 100, pp. 223-230.

Meneghini, J.R., 2002, Projetos de pesquisa no tópico geração e desprendimento de vórtices no escoamento ao redor de cilindros, Livre Docência, Escola Politécnica da Universidade de São Paulo, São Paulo.

Nishimoto, K., 1985, Assessment of safety design for offshore structures in ocean environment forces. Dissertation (Doctor) - University of Tokyo, Departament of Naval Architecture, 2v.

Omega Engineering, 2004, The Strain Gage, EUA, http://www.omega.com/literature/transactions/volume3/strain2.html.

10. Responsibility notice

The authors are the only responsibles for the printed material included in this paper.